CROATICA CHEMICA ACTA
CCACAA, ISSN-0011-1643, ISSN-1334-417X

Croat. Chem. Acta **82** (2) (2009) 469–476
CCA-3337

Review

Hydrogen Sorption Properties of Some $RM_{2-x}M'_x$ and $RM_{2-x}Al_x$ (R = Y, Gd, Tb, Er, Ho; M = Mn, Fe, Co, Ni) Laves Phase Ternary Compounds*

Bohdan Kotur,[a,] Oksana Myakush,[a] and Ihor Zavaliy[b]**

[a]*Department of Inorganic Chemistry, Ivan Franko National University of Lviv, Kyryla & Mefodiya Str. 6, UA-79005 Lviv, Ukraine*

[b]*Physico-Mechanical Institute of NAS of Ukraine, Naukova Str. 3, Lviv, UA-79601, Ukraine*

RECEIVED JULY 22, 2008; REVISED JANUARY 8, 2009; ACCEPTED JANUARY 13, 2009

Abstract. A literature and authors' review of influence of hydrogen absorption on the crystal structure of binary RM_2 and ternary $RM_{2-x}M'_x$, $R_{1-x}R'_xNi_2$ and $RM_{2-x}Al_x$, (R = Rare earth; M = Mn, Fe, Co, Ni) Laves phase compounds are presented. Majority of these compounds absorb hydrogen at pressure 0.1–0.12 MPa and room temperature preserving the crystalline state. The phases form hydrides with the amount of hydrogen up to 4.2 atoms H per formula unit (at.H/f.u.) and up to 5 at.H/f.u. at high hydrogen pressure. The unit cell volume increases under hydrogenation up to 20 % and up to 30 % at high hydrogen pressure. In many cases the doping of binary phases by the third element increases hydrogenation capacity of intermetallics under the same hydrogenation conditions. The structure of the parent compound is preserved or slightly distorted during hydrogenation.

Keywords: Laves phases, hydrides, crystal structure

THE HYDRIDES BASED ON RM_2 (M = Mn, Fe, Co, Ni) COMPOUNDS

The influence of hydrogen absorption on the structure and physical properties of the RM_2 (R = Rare earth metal; M = Mn, Fe, Co, Ni) Laves phase compounds has been widely studied with the aim of their hydrides application in the production of magnets, metal hydride electrodes, hydrogen accumulators, *etc*.[1–5] These compounds can easily absorb large amount of hydrogen into interstitial tetrahedral sites of their crystal structure. The neutron diffraction analysis of RM_2H_x deuterides[6] shows that the deuterium atoms are located in tetrahedral interstitial sites with a maximum content in the R rich site (active hydride-forming element), *i.e.* first in R_2M_2 and then in RM_3 tetrahedra. In the RM_2 Laves phases the hydrogen content can be varied up to 5 atoms per formula unit (at.H/f.u.) leading to a cell volume increase up to 30 %.[7] Hydrogenation is usually accompanied by a decrease of the crystal symmetry.

The RMn_2 intermetallic compounds crystallize either in the hexagonal $MgZn_2$ type structure for R = Pr, Nd, Sm, Er, Tm and Lu or in the cubic $MgCu_2$ type for R = Y, Gd, Tb, Dy and Ho.[8] These compounds absorb hydrogen up to 4.3–4.5 at.H/f.u. when hydrogen pressure is limited to moderate values. Their unit cell is expanded proportionally with the hydrogen content, which has been already reported for YMn_2H_x,[9–15] $GdMn_2H_x$,[16] $TbMn_2H_x$,[17] $DyMn_2H_x$,[15] $ErMn_2H_x$,[18] $SmMn_2H_2$,[19] $HoMn_2H_x$.[20] The structural transformations of the RMn_2H_x hydrides are strongly related to the hydrogen concentration. Up to now YMn_2H_x is the most investigated system. It was found, that for hydrogen concentrations of $0.3 < x < 1.1$ the hydrides RMn_2H_x undergo a tetragonal distortion, similar to the one observed for YMn_2.[12] In the concentration range $1.2 \le x \le 3.5$ the cubic Laves phase structure of the $MgCu_2$ type is preserved in the whole temperature range. For the high hydrogen concentration $x > 3.5$ it is not possible to obtain a single-phase hydride at room temperature, and one can observe the co-existence of cubic and tetragonal hydride phases[15] or rhombohedral type phases.[13] In the concentration range $4.1 \le x \le 4.5$ the rhombohedral structure (*R*-3*m* space group) was observed.[13,14] A new phase of $ErMn_2D_6$ has been synthesized by applying 50 MPa hydrogen pressure on C14 $ErMn_2$. This phase is isostructural to YMn_2D_6 and

* Dedicated to Professor Emeritus Drago Grdenić, Fellow of the Croatian Academy of Sciences and Arts, on the occasion of his 90th birthday.

** Author to whom correspondence should be addressed. (E-mail: kotur@franko.lviv.ua)

crystallizes with K_2PtCl_6 type of structure.[21] The structural investigations of the RMn_2H_x (R = Sm, Gd, Tb, Dy, Er, Ho) hydrides display some common features, depending on hydrogen content:

a) no tetragonal distortion occurs for low H ($x < 0.2$) content;

b) decomposition of a sample of spinodal type into two hydride phases with lower and higher hydrogen content x is observed;

c) the single phase hydrides with the $MgCu_2$ or $MgZn_2$ (for R = Sm, Er) structure are preserved in the range $1 \le x \le 3.5$;

d) for the hydrogen concentration range $3.5 < x < 4.3$ coexistence of cubic $MgCu_2$-type structure and rhombohedral phases with various ratios or two $MgZn_2$-type phases (for R = Sm, Er) are observed;

e) for the $RMn_2H_{4.3}$ hydrides, the same type of rhombohedral structure occurred;

f) for high hydrogen pressure (10 kbar) RMn_2H_6 phases occur with completely different structure, *i.e.* complex like, compared to those which are derived from the C15 ($MgCu_2$) or C14 ($MgZn_2$) phases (points a) – e)).

The type of Rare earth and temperature influence the hydrogen induced phase transformations. The main exceptions were observed for RMn_2 (R = Sm and Er) which crystallize in C14-type structure.

All existing RFe_2 compounds crystallize in the cubic $MgCu_2$ type structure. The RFe_2 compounds are interesting due to their ability to form RFe_2H_x hydrides with concentrations ranging from 1.2 to 5 at.H/f.u.[22,23] The structural changes in the cubic Laves phases RFe_2 are particularly interesting, because both crystalline (c-) and amorphous (a-) hydrides can be obtained depending on the hydrogenation conditions. The authors of the works[24,25] investigated the process and mechanism of hydrogen-induced amorphization in C15 Laves phases RFe_2 (R = Y, Ce, Sm, Gd, Tb, Dy, Ho and Er). Hydrogen absorption in the crystalline state, hydrogen-induced amorphization, precipitation of RH_2 and finally decomposition of the remaining amorphous phase into RH_2 and α-Fe with increasing the temperature were observed in RFe_2 (R = Y, Sm, Gd, Tb, Dy and Ho). Crystalline hydride $CeFe_2H_x$ is not formed. Hydrogen-induced amorphization in YFe_2 occurs in two stages: c-$YFe_2H_x \rightarrow$ (1st stage) c-YFe_2H_{x-y} + a-$YFe_2H_x \rightarrow$ (2nd stage) a-YFe_2H_x. The formation of the crystalline hydrides at ambient temperatures has been reported too. For example, in the process of formation of the hydrides YFe_2H_x hydrogen (deuterium) absorption induced the formation of several single phase YFe_2H_x hydrides with different structures derived from the $MgCu_2$ Laves phase: $YFe_2H_{1.2}$ (tetragonal, space group I-4), $YFe_2H_{1.75}$ (cubic, space group I-43m), $YFe_2H_{1.9}$ (cubic, primitive lattice), $YFe_2H_{2.5-2.9}$ (cubic, space group Fd-3m), $YFe_2H_{3.5-4.2}$ (rhombohedral, space group R-3m).[22,26,27] Recently the same group of authors[28,29] reported also a monoclinic superstructure (space group $C2/m$) for $YFe_2D_{3.5}$ and $YFe_2(H_yD_{1-y})_{4.2}$. An orthorhombic structure has been reported for YFe_2H_5 and $ErFe_2H_5$.[30,31] The RFe_2H_x compounds (R = Gd, Tb, Ho, Er, Tm, Lu) adopt the $MgCu_2$ type structure in the concentration region $1.2 < x < 3.0$ and in the rhombohedral structure above 3–3.5 at.H/f.u.[7,10,23,25,32]

Similar to RFe_2 compounds, all existing RCo_2 compounds crystallize in the cubic $MgCu_2$ type structure. The results of the works[1,33–35] demonstrated that RCo_2 compounds (R = Nd, Gd, Tb, Dy, Ho, Er) absorb hydrogen up to 3.0–4.0 at.H/f.u and structure of the basic compounds and their hydrides is the same. The RCo_2 compounds (R = Y, La, Pr) change their crystal structure after hydrogenation. The $SmCo_2$ compound forms two hydrides $SmCo_2H_3$ ($MgCu_2$ type stucture)[36] and $SmCo_2H_4$ ($MgZn_2$ type structure).[37]

First publications on the binary RNi_2 compounds indicated that they belong to the cubic Laves phase ($MgCu_2$ structure type).[38] However, the authors[39–45] pointed out that these compounds have a structure derived from the ideal cubic $MgCu_2$ structure with defect composition $R_{1-x}Ni_2$ and a $TmNi_2$ structure type (α phase) (with doubled a lattice parameter). The vacancies of the R atoms sublattice depend on the radius of Rare earth.[40] The first detailed analysis of this superstructure was performed for YNi_2, showing that a single phase compound can be obtained only with the stoichiometry 0.95 : 2 and can be described within a space group F-43m with the 4a sites only partially occupied by the Y atoms.[45] The systematic investigation of the $R_{1-x}Ni_2$ compounds revealed that this superstructure exists also for other R elements, however, the occupancy of the 4a sites increases with decreasing radius of the R atom and reaches 1 for $LuNi_2$.[39] These compounds form hydrides which are crystalline or amorphous depending on the absorption conditions and on the atomic radius of the rare earth atom. Aoki *et. al.*[46,47] reported the formation of amorphous RNi_2 hydrides for R = La, Ce, Pr, Sm, Gd, Tb, Dy, Ho and Er. For $La_{0.92}Ni_2$ and $Ce_{0.95}Ni_2$ it was observed that the α phase transforms directly into an amorphous hydride.[45] For $Nd_{0.95}Ni_2$ the formation of a crystalline hydride is observed but it transforms into an amorphous phase and there is a competition between these two hydrides formation.[39] For $Y_{0.95}Ni_2$, $Tb_{0.95}Ni_2$ and $Er_{0.98}Ni_2$ a crystalline hydride is obtained for 2.5 at.H/f.u.[39,42] It preserves the structure of the parent

intermetallic with $\Delta V/V$ of about 18 %. The $Tb_{0.95}Ni_2$ forms another crystalline hydride (γ phase) with $\Delta V/V =$ 27 % and an amorphous hydride.[39]

During last years we studied a number of binary Laves phases RM_2 doped with the third component in order to investigate the influence of the doping element on hydrogenation abilities of alloys. These results and the experimental procedure are presented in detail in[48–59] and are generalized briefly below. The parent alloys were arc melted in argon atmosphere from the initial components. The hydrides were synthesized at room temperature under 0.12 MPa hydrogen pressure in autoclave after preliminary activation of the samples in vacuum at 350–400 °C. The amount of absorbed hydrogen was determined volumetrically. X-ray powder diffraction (Rietveld profile analysis) has been used to study the phase composition of parent alloys and their hydrides. Thermal decomposition of hydrides has been studied in vacuum and hydrogen atmosphere.

THE HYDRIDES BASED ON $ErM_{2-x}M'_x$ (M = Fe, Co; M' = Ti, V, Cr, Mn, Ni, Cu, Mo) COMPOUNDS

All investigated $ErFe_{2-x}M_x$ (M = Ti, V, Cr, Mn, Co, Ni, Cu, Mo) samples absorb a large amount of hydrogen (≈ 3.5–4.0 at.H/f.u.) without amorphization.[48–51] Hydrogenation of the $ErFe_2$ is accompanied by phase transition of the cubic $MgCu_2$-type structure into the rhombohedral one of the $TbFe_2$ type. Substitution of Fe ($r = 0.1241$ nm) by low amounts (5 at.%) of 3*d*-metal with the similar atomic radius (Cr, r = 0.1249 nm; Co, $r = 0.1253$ nm; Ni, r = 0.1246 nm; Cu, r = 0.1278 nm) decreases the hydrogen storage capacity of the alloys (*e.g.* from 3.8 at.H/f.u. for $ErFe_2$ to 3.5 at.H/f.u. for $ErFe_{2-x}Cu_x$). Hydrogenation of these ternary alloys is accompanied by the phase transition of the cubic structure ($MgCu_2$-type) into the rhombohedral one ($TbFe_2$-type) as it occurs in the case of the basic compound $ErFe_2$. Substitution of Fe by larger atom (Ti, r = 0.1448 nm; V, r = 0.1321 nm; Mo, r = 0.1362 nm) increases the hydrogenation capacity of the $ErFe_{2-x}M_x$ compounds. The structure of the parent compounds and their hydrides remains the same. Crystallographic parameters of the $ErFe_{1.85}M_{0.15}$ (M = Ti, V, Cr, Mn, Co, Ni, Cu, Mo) compounds and their hydrides are presented in Table 1.

The existence of the solid solutions $ErFe_{2-x}V_x$ ($0 \le x \le 0.23$) and $ErCo_{2-x}V_x$ ($0 \le x \le 0.33$) with the $MgCu_2$-type structure in the Er-{Fe, Co}-V ternary systems has been reported in References 49, 51, 52. These samples absorb relatively large amounts of hy-

Table 1. Crystallographic parameters of the $ErFe_{1.85}M_{0.15}$ (M = Ti, V, Cr, Mn, Co, Ni, Cu, Mo) alloys and their hydrides

Alloys and their hydrides	Structure type	Lattice parameters				H/M[(b)]
		a / nm	c / nm	V / nm^3	$(\Delta V/V)^{(a)}$ / %	
$ErFe_2$	$MgCu_2$	0.7285(1)		0.3865(1)		
$ErFe_2H_{3.8}$	$TbFe_2$	0.5594(2)	1.3286(6)	0.3589(4)		1.27
$ErFe_{1.85}Ti_{0.15}$	$MgCu_2$	0.7382(1)		0.4023(1)		
$ErFe_{1.85}Ti_{0.15}H_{4.0}$	$MgCu_2$	0.7916(1)		0.4960(1)	23.29	1.33
$ErFe_{1.85}V_{0.15}$	$MgCu_2$	0.7298(1)		0.3887(1)		
$ErFe_{1.85}V_{0.15}H_{3.9}$	$MgCu_2$	0.7877(1)		0.4887(1)	25.73	1.30
$ErFe_{1.85}Cr_{0.15}$	$MgCu_2$	0.7288(1)		0.3871(1)		
$ErFe_{1.85}Cr_{0.15}H_{3.8}$	$TbFe_2$	0.5591(2)	1.3305(6)	0.3601(3)		1.27
$ErFe_{1.85}Mn_{0.15}$	$MgCu_2$	0.7284(1)		0.3864(1)		
$ErFe_{1.85}Mn_{0.15}H_{3.9}$	$MgCu_2$	0.7852(1)		0.4842(1)	25.31	1.30
$ErFe_{1.85}Co_{0.15}$	$MgCu_2$	0.7279(1)		0.3857(1)		
$ErFe_{1.85}Co_{0.15}H_{3.6}$	$TbFe_2$	0.5571(2)	1.3228(5)	0.3554(3)		1.20
$ErFe_{1.85}Ni_{0.15}$	$MgCu_2$	0.7276(1)		0.3852(1)		
$ErFe_{1.85}Ni_{0.15}H_{3.5}$	$TbFe_2$	0.5536(2)	1.3299(7)	0.3530(3)		1.17
$ErFe_{1.85}Cu_{0.15}$	$MgCu_2$	0.7291(1)		0.3875(1)		
$ErFe_{1.85}Cu_{0.15}H_{3.5}$	$TbFe_2$	0.5567(2)	1.3331(5)	0.3578(2)		1.17
$ErFe_{1.85}Mo_{0.15}$	$MgCu_2$	0.7309(1)		0.3905(1)		
$ErFe_{1.85}Mo_{0.15}H_{4.0}$	$MgCu_2$	0.7881(1)		0.4893(1)	25.30	1.33

[(a)]$\Delta V/V$ = (V(hydride) – V(parent alloy)) / V(parent alloy)) × 100; V – unit cell volume
[(b)]H/M - atoms of H per metal atom in the structure of hydride

Table 2. Crystallographic and hydrogenation properties of the $ErCo_{2-x}V_x$ and $ErFe_{2-x}V_x$ alloys ($MgCu_2$ type structure)

Alloys and their hydrides	Lattice parameters			H/M
	a / nm	*V* / nm^3	(Δ*V*/*V*) / %	
$ErCo_2$	0.71559(5)	0.36644(8)		
$ErCo_2H_{3.7}$	0.7618(2)	0.4421(4)	20.65	1.23
$ErCo_{1.85}V_{0.15}$	0.71773(5)	0.3697 (8)		
$ErCo_{1.85}V_{0.15}H_{3.8}$	0.7670(7)	0.4510 (1)	22,0	1,27
$ErCo_{1.76}V_{0.24}$	0.71896(7)	0.37164(1)		
$ErCo_{1.76}V_{0.24}H_{3.8}$	0.7728(2)	0.4615(3)	24.18	1.27
$ErCo_{1.67}V_{0.33}$	0.71976(5)	0.37288(8)		
$ErCo_{1.67}V_{0.33}H_{3.8}$	0.7746(1)	0.4647(3)	24.62	1.27
$ErFe_{1.90}V_{0.10}$	0.72892(7)	0.3882(1)		
$ErFe_{1.90}V_{0.10}H_{3.8}$	0.7869(1)	0.4872(1)	25.50	1.27
$ErFe_{1.85}V_{0.15}$	0.7298(1)	0.3887(1)		
$ErFe_{1.85}V_{0.15}H_{3.9}$	0.7877(1)	0.4887(1)	25.73	1.30
$ErFe_{1.78}V_{0.22}$	0.73125(7)	0.3910(4)		
$ErFe_{1.78}V_{0.22}H_{4.2}$	0.7915(1)	0.4958(3)	26.80	1.40

drogen from 3.7 to 4.2 at.H/f.u. without amorphization.[48,52] All hydrides preserve the structure of the parent metallic matrix. As it is seen from the data presented in the Tables 1 and 2, the substitution of iron by vanadium causes significant increase of the hydrogen-sorption capacity of alloys from 3.8 at.H/f.u. for $ErFe_2$ to 4.2 at.H/f.u. for $ErFe_{1.78}V_{0.23}$ whereas the substitution of cobalt by vanadium influences the hydrogenation capacity of the samples slightly (Table 2).

THE HYDRIDES BASED ON RNi_2 (R = Y, Gd, Er) BINARY COMPOUNDS WITH THE R BY R', Ni BY Fe AND Ni BY V SUBSTITUTIONS

Our previous publications[53–55] were focused on the investigation of the influence of the substitution of Ni by Fe and V and of Er by Y on the crystal structure, hydrogenation properties and kinetic of the hydrogenation-dehydrogenation process of the alloys based

Table 3. Crystallographic and hydrogen sorption characteristics of the RNi_2 (R = Y, Gd, Er) binary compounds, $R_{1-x}R'_xNi_2$, $RNi_{2-x}Fe_x$, $ErNi_{2-x}V_x$ alloys and their hydrides

Alloys and their hydrides	Structure type	Lattice parameters			H/M
		a / nm	*V* / nm^3	(Δ*V*/*V*) / %	
$GdNi_2$	$TmNi_2$	1.44085(8)	2.991.2(3)	–	–
$GdNi_2H_{3.2}$	$TmNi_2$	1.5221(11)	3.526(4)	17.9	1.07
$Gd_{0.85}Y_{0.15}Ni_2$	$TmNi_2$	1.44017(7)	2.9870(2)	–	–
$Gd_{0.85}Y_{0.15}Ni_2H_{3.6}$	$TmNi_2$	1.5209(9)	3.5180(4)	17.8	1.20
$GdNi_{1.85}Fe_{0.15}$	$MgCu_2$	0.72246(3)	0.37709(3)	–	–
$GdNi_{1.85}Fe_{0.15}H_{3.8}$	$MgCu_2$	0.7674(11)	0.452(2)	19.9	1.27
$ErNi_2$	$TmNi_2$	1.42678(6)	2.9045(2)	–	–
$ErNi_2H_{3.0}$	$TmNi_2$	1.4997(4)	3.3730(14)	16.1	1.00
$Er_{0.85}Y_{0.15}Ni_2$	$TmNi_2$	1.42920(6)	2.9193(2)	–	–
$Er_{0.85}Y_{0.15}Ni_2H_{3.4}$	$TmNi_2$	1.5010(4)	3.3816(15)	15.8	1.13
$ErNi_{1.85}Fe_{0.15}$	$MgCu_2$	0.71707(3)	3.6871(3)	–	–
$ErNi_{1.85}Fe_{0.15}H_{3.3}$	$MgCu_2$	0.7490(4)	0.4201(4)	13.9	1.10
$ErNi_{1.85}V_{0.15}$	$TmNi_2$	1.4258(3)	2.8988(4)		
$ErNi_{1.85}V_{0.15}H_{3.2}$	$TmNi_2$	1.5000(1)	3.3750(5)	16.42	1.07
YNi_2	$TmNi_2$	1.43575(9)	2.9596(3)	–	–
$YNi_2H_{3.1}$	$TmNi_2$	1.5107(3)	3.4478(12)	16.5	1.03

on $ErNi_2$ binary compound. The results of the investigation of the hydrogenation properties of the $R_{0.85}Y_{0.15}Ni_2$, $RNi_{1.85}Fe_{0.15}$ (R = Gd and Er) and RNi_2 (R = Y, Gd and Er) are presented in detail in Ref. 56.

The Fe-containing alloys $GdNi_{1.85}Fe_{0.15}$ and $ErNi_{1.85}Fe_{0.15}$ adopt the $MgCu_2$ type structure, however $R_{0.85}Y_{0.15}Ni_2$ (R = Gd and Er) and RNi_2 (R = Y, Gd and Er) crystallize with the $TmNi_2$ cubic structure with doubled cell parameter *a*. The doubling of the cell parameter in $R_{1-x}Ni_2$ or $(R, R')_{1-x}Ni_2$ compounds is related to ordered R vacancies. Therefore the substitution of Ni by Fe either cancels the R vacancies or induces the ordering of the vacancies. These data are summarized in Table 3. The above mentioned phases absorb 3.0–3.8 at.H/f.u. with the increasing cell volume up to 20 %. Hydrides of these Laves phases preserve the crystal structure of the parent compound (Table 3). The crystal structure was refined for $Er_{0.85}Y_{0.15}Ni_2H_{3.4}$ hydride.[54,55] Under the same hydrogenation conditions ternary substituted phases absorb more hydrogen in comparison with the binary compounds as it is seen from Figure 1. The hydrogen storage capacity of the $GdNi_{1.85}Fe_{0.15}H_{3.8}$ hydride is the highest one in the series and is equal to 1.27 H/M.

Hydrogen desorption curves for the hydride phases $ErNi_2H_{3.0}$, $Er_{0.85}Y_{0.15}Ni_2H_{3.4}$, $ErNi_{1.85}V_{0.15}H_{3.2}$ heated in hydrogen and argon atmosphere with speed of 5 K/min are presented in Figure 2. An intensive hydrogen release begins already at ≈ 120–130 ºC. We suppose that this temperature indicates that hydrogen desorbs from RM_3 interstitial tetrahedral sites of the structure. The width of the first peak on dehydrogenation curves for $ErNi_{1.85}V_{0.15}H_{3.2}$ hydride is the evidence of higher hydro-gen content in the RM_3 tetrahedral sites in this hydride in comparison with the $ErNi_2H_{3.0}$ and $Er_{0.85}Y_{0.15}Ni_2H_{3.4}$ hydrides. Substitution of Ni (r = 1.24 Å) by the larger atom V (r = 1.34 Å) increases the dimension of the interstitial tetrahedral sites of the structure and increases the hydrogenation capacity of the

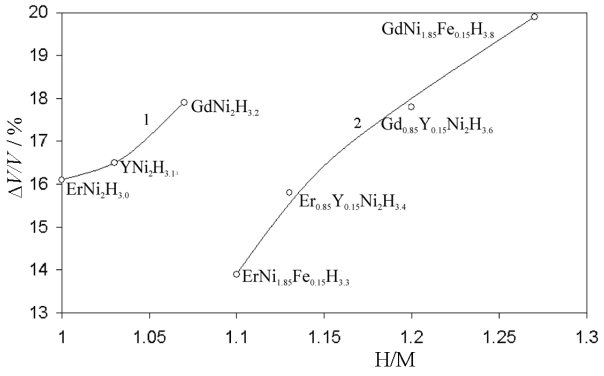

Figure 1. Dependence of $\Delta V/V$ *vs.* H/M for the binary (1) and tertiary (2) hydrides.

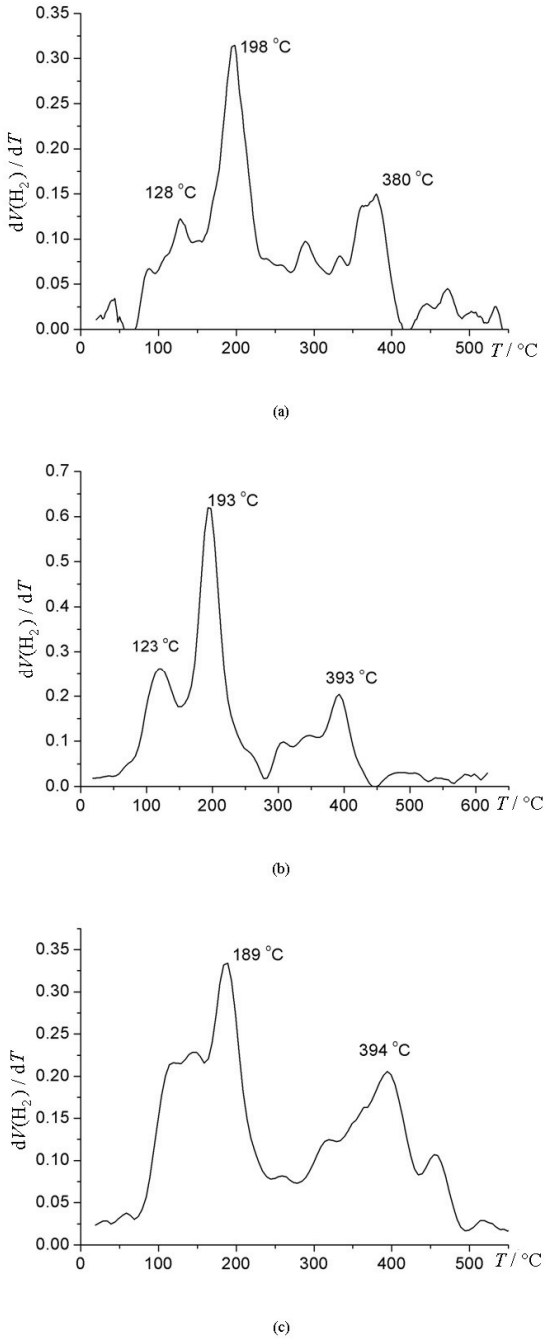

Figure 2. Hydrogen desorption curves for $ErNi_2H_{3.0}$ (a), $Er_{0.85}Y_{0.15}Ni_2H_{3.4}$ (b), $ErNi_{1.85}V_{0.15}H_{3.2}$ (c) hydrides.

$ErNi_{1.85}V_{0.15}$ compound. The hydrogen desorption traces indicate two main peaks of hydrogen desorption from R_2M_2 tetrahedral sites occurring at around 200 and 400 °C. The substitution of Ni by V and of Er by Y reduces the temperature of desorption of the main part of hydrogen from 198 ºC for $ErNi_2H_{3.0}$ to 189 ºC for $ErNi_{1.85}V_{0.15}H_{3.2}$ and to 193 ºC for $Er_{0.85}Y_{0.15}Ni_2H_{3.4}$ and increases the temperatures of desorption of the remaining hydrogen from 380 ºC for $ErNi_2H_{3.0}$ to 394 ºC for $ErNi_{1.85}V_{0.15}H_{3.2}$ and to 393 ºC for $Er_{0.85}Y_{0.15}Ni_2H_{3.4}$.

Table 4. Crystallographic and hydrogen sorption characteristics of the $RM_{2-x}Al_x$ (R = Gd, Tb, Ho; M = Mn, Fe) alloys and their hydrides

Alloys and their hydrides	Structure type	Lattice parameters				H/M
		a / nm	*c* / nm	*V* / nm^3	($\Delta V/V$) / %	
$TbFe_{1.70}Al_{0.30}$	$MgCu_2$	0.74283(3)		0.4099(2)		
$TbFe_{1.70}Al_{0.30}H_{3.2}$	$MgCu_2$	0.79191(3)		0.4967(3)	21.2	1.07
$TbFe_{1.55}Al_{0.45}$	$MgCu_2$	0.74618(3)		0.4155(2)		
$TbFe_{1.55}Al_{0.45}H_{3.0}$	$MgCu_2$	0.78943(2)		0.4920(2)	18.4	1.00
$TbFe_{1.25}Al_{0.75}$	$MgZn_2$	0.53435(4)	0.87170(7)	0.2156(4)		
$TbFe_{1.25}Al_{0.75}H_{2.4}$	$MgZn_2$	0.55254(3)	0.91658(5)	0.2423(4)	11.4	0.80
$TbFe_{1.10}A_{10.90}$	$MgZn_2$	0.53776(4)	0.87419(7)	0.2189(4)		
$TbFe_{1.10}Al_{0.90}H_{2.3}$	$MgZn_2$	0.55131(3)	0.91246(5)	0.2402(3)	9.7	0.77
$GdMn_{1.85}Al_{0.15}$	$MgCu_2$	0.7806(1)		0.4756(1)		
$GdMn_{1.85}Al_{0.15}H_{4.2}$	$MgCu_2$	0.8207(1)		0.5528(1)	16.2	1.40
$GdMn_{1.50}Al_{0.50}$	$MgCu_2$	0.7838(1)		0.4815(1)		
$GdMn_{1.50}Al_{0.50}H_{3.4}$	$MgCu_2$	0.8069(1)		0.5254(1)	9.1	1.13
$TbMn_{1.85}Al_{0.15}$	$MgCu_2$	0.7708(1)		0.4579(1)		
$TbMn_{1.85}Al_{0.15}H_{4.3}$	$MgCu_2$	0.8164(1)		0.5441(1)	18.8	1.43
$TbMn_{1.50}Al_{0.50}$	$MgCu_2$	0.7761(1)		0.4675(1)		
$TbMn_{1.50}Al_{0.50}H_{3.5}$	$MgCu_2$	0.8053 (1)		0.5222(1)	11.7	1.17
$HoFe_{1.6}Al_{0.4}$	$MgCu_2$	0.73853(2)	–	0.4028(2)		
$HoFe_{1.6}Al_{0.4}H_{3.0}$	$MgCu_2$	0.78063(4)	–	0.4757(1)	18.1	1.00
$HoFe_{1.2}Al_{0.8}$	$MgZn_2$	0.53042(8)	0.86614(8)	0.2111(6)		
$HoFe_{1.2}Al_{0.8}H_{2.4}$	$MgZn_2$	0.54679(8)	0.9047(2)	0.2343(1)	11.0	0.80

The stability of the hydrides based on $ErNi_2$ compound increases with the substitution of Er by Y. The $ErNi_2H_{3.0}$, $Er_{0.85}Y_{0.15}Ni_2H_{3.4}$, $ErNi_{1.85}V_{0.15}H_{3.2}$ hydrides totally desorbed hydrogen at temperatures ≈ 380–394 ºC. After dehydrogenation these samples returned to the structure of the initial compounds. The hydrogen desorption process needs additional structural investigations (XRD or better NPD) of samples annealed at temperatures before and after each peak.

THE HYDRIDES BASED ON $RM_{2-x}Al_x$ (R = Gd, Tb, Ho; M = Mn, Fe) COMPOUNDS

The existence of the solid solutions $RM_{2-x}Al_x$ with the $MgCu_2$ and $MgZn_2$ type structures in the R-M-Al (R = Gd, Tb, Ho; M = Mn, Fe) ternary systems has been reported.[57] The influence of aluminum content on hydrogenation properties of these phases has been studied.[58,59] These summarized data are presented in Table 4. It is shown that hydrides retain initial structure of metal matrix with maximum expansion of unit cell volume up to 18.8 %. Similar to the $CeMn_{2-x}Al_x$[60–62] and $ErM_{2-x}Al_x$ (M = Fe, Co, Ni)[63,64] alloys for the $RM_{2-x}Al_x$ (R = Gd, Tb, Ho; M = Mn, Fe) series the decrease of hydrogen storage capacity as a function of increasing Al content has been observed.[58,59]

CONCLUSIONS

Binary RM_2 (R = Rare earth metal; M = Mn, Fe, Co, Ni) Laves phase compounds can easily absorb large amount of hydrogen up to 3.0–4.2 at.H/f.u. at 0.1–0.12 MPa pressure. At pressure ≈ 20 MPa the hydrogen content can be increased continuously or by steps up to 5 at.H/f.u. leading to a cell volume increase up to 30 %. Hydrogenation is accompanied in some cases by the decrease of the crystal symmetry due to hydrogen ordering and at higher temperatures by the processes of amorphization, spinodal decomposition or precipitation. The deuterides with 6 at.D/f.u. capacity have been synthesized at 50 MPa pressure for RMn_2 (R = Y, Er). Their crystal structure is a complex like one and is completely different from those which are derived from the C15 or C14 phases.

Binary Laves phases RM_2 doped with the third component absorb up to ≈ 4.2 at.H/f.u. at 0.10–0.12 MPa pressure. The partial substitution of 3*d*-element by larger atom Ti, V, Mo increases hydrogen storage capacity of compounds: *e.g.* for $ErFe_{2-x}V_x$ solid solution it increases from 3.8 at.H/f.u. for $x = 0$ to 4.2 at.H/f.u. for $x = 0.22$. All ternary $R_{1-x}R'_xNi_2$, $RNi_{2-x}Fe_x$ and $RNi_{2-x}V_x$ phases based on RNi_2 (R = Y, Gd, Er) absorb more hydrogen in comparison with

the initial binary compounds, whereas the substitution of *d*-element by *p*-element (Al) linearly decreases hydrogen absorption capacity of intermetallic with increasing x in the $RM_{2-x}Al_x$ (R = Gd, Tb, Ho; M = Mn, Fe) alloys.

The hydrides of the $ErCo_{2-x}V_x$ ($MgCu_2$-type structure), $R_{1-x}R'_xNi_2$, $RNi_{2-x}Fe_x$ and $RNi_{2-x}V_x$ (R = Y, Gd, Er) ($MgCu_2$ or $TmNi_2$-type structure), $RM_{2-x}Al_x$ (R = Gd, Tb, Ho; M = Mn, Fe) ($MgCu_2$ or $MgZn_2$-type structures) alloys preserve the structure of the original metallic matrix. Hydrogenation of the $ErFe_{2-x}M_x$ compounds (M = Cr, Co, Ni, Cu – a 3*d*-metal with the similar to Fe atomic radius) is accompanied by the phase transition of the cubic structure ($MgCu_2$-type) into the rhombohedral one ($TbFe_2$-type) as it occurs in the case of the basic compound $ErFe_2$. Substitution of Fe by the larger atom (Ti, r = 0.1448 nm; V, r = 0.1321 nm; Mo, r = 0.1362 nm) increases the hydrogenation capacity of the $ErFe_{2-x}M_x$ compounds. Structure of the parent compounds $ErFe_{2-x}M_x$ (M = Ti, V, Mo - metal with the larger than Fe atomic radius) and their hydrides remain the same for low hydrogen pressures.

REFERENCES

1. K. H. G. Buschow, *Hydrogen absorption in intermetallic compounds*, in: K. A. Gschneidner, Jr. and L. Eyring (Eds.), *Handbook on the Physics and Chemistry of Rare Earths*, Vol. 10, North–Holland Publishing Co., 1984, pp. 1–111.
2. V. Guther and A. Otto, *J. Alloys Compd*. **293**–**295** (1999) 889–892.
3. K. Yvon and P. Fischer, *Crystal and Magnetic Structures of Ternary Metal Hydrides: A Comprehensive Review*, in: *Topics in Applied Physics*, Vol.63. *Hydrogen in Intermetallic Compounds I. Electronic, Thermodynamic, and Crystallographic Properties, Preparation*, Springer–Verlag, Berlin, 1988, pp. 87–138.
4. D. Shaltiel, *J. Less–Common Met.* **62** (1978) 407–416.
5. V. V. Burnasheva, A. V. Ivanov, and K. N. Semenenko, *Izv. AN SSSR, Inorganic Mater.* **14** (1978) 1302–1307.
6. K. Itoh, K. Kanda, R. Aoki, and T. Fukunaga, *J. Alloys Compd.* **348** (2003) 167–172.
7. V. Paul-Boncour, S. M. Filipek, A. Percheron-Guegan, I. Marchuk, and J. Pielaszek, *J. Alloys Compd.* **317**–**318** (2001) 83–87.
8. H. R. Kirchmayr and W. Lugscheider, *Z. Metallkd.* **58** (1967) 185–188.
9. J. Przevoznik, V. Paul–Boncour, M. Latroche, and A. Percheron-Guegan, *J. Alloys Compd.* **232** (1996) 107–118.
10. V. Paul–Boncour, *J. Alloys Compd.* **367** (2004) 185–190.
11. H. Figiel, J. Przewoznik, V. Paul-Boncour, A. Lindbaum, E. Gratz, M. Latroche, M. Escorne, A. Percheron-Guégan, and P. Mietniowski, *J. Alloys Compd.* **274** (1998) 29–37.
12. H. Fujii, M. Saga, and T. Okamoto, *J. Less–Common Met.* **130** (1987) 25–31.
13. I. N. Goncharenko, I. Mirebeau, A. V. Irodova, and E. Suard, *Phys. Rev. B.* **56** (1997) 2580–2584.
14. M. Latroche, V. Paul-Boncour, A. Perchéron-Guegan, and F. Bouree-Vigneron, *J. Alloys Compd.* **274** (1998) 59–64.
15. J. Przewoznik, J. Zukrowski, K. Freindl, E. Japa, and K. Krop, *J. Alloys Compd.* **284** (1999) 31–41.
16. J. Zukrowski, H. Figiel, A. Budziak, P. Zachariasz, G. Fischer, M. T. Kelemen, and E. Dormann, *J. Magn. Magn. Mater.* **238** (2002) 129–139.
17. H. Figiel, A. Budziak, J. Zukrowski, G. Fischer, M. T. Kelemen, and E. Dormann, *J. Alloys Compd.* **335** (2002) 48–58.
18. H. Figiel, A. Budziak, P. Zachariasz, J. Zukrowski, G. Fischer, and E. Dormann, *J. Alloys Compd.* **368** (2004) 260–268.
19. H. Figiel, A. Budziak, and J. Zukrowski, *Solid State Commun.* **111** (1999) 519–524.
20. Z. Tarnawski, L. Kolwicz-Chodak, H. Figiel, N. T. H. Kim-Ngan, A. Kozlowski, T. Dawid, L. Havela, K. Miliyanchuk, and E. Santava, *J. Alloys Compd.* **446**–**447** (2007) 415–418.
21. V. Paul-Boncour, S. M. Filipek, G. Andre, F. Bourée, M. Guillot, R. Wierzbicki, I. Marchuk, R. S. Liu, B. Villeroy, A. Perchéron-Guegan, H. D. Yang, and S. C. Pin, *J. Phys.: Condens. Matter* **18** (2006) 6409–6420.
22. V. Paul-Boncour, L. Guénée, M. Latroche, B. Ouladdiaf, and F. Bouree-Vigneron, *J. Solid State Chem.* **142** (1999) 120–129.
23. D. Fruchart, Y. Berthier, T. de Saxce, and P. Vulliet, *J. Solid State Chem.* **67** (1987) 197–209.
24. M. Dilixiati, K. Kanda, K. Ishikawa, and K. Aoki, *J. Alloys Compd.* **337** (2002) 128–135.
25. K. Aoki, H.-W. Li, and K. Ishikawa, *J. Alloys Compd.* **404**–**406** (2005) 559–564.
26. V. Paul-Boncour, L. Guénée, M. Latroche, M. Escorne, A. Perchéron-Guegan, Ch. Reichl, and G. Wiesinger, *J. Alloys Compd.* **253**–**254** (1997) 272–274.
27. V. Paul–Boncour and A. Perchéron–Guegan, *J. Alloys Compd.* **293**–**295** (1999) 237–242.
28. V. Paul-Boncour, M. Guillot, G. Wiesinger, and G. Andre, *Phys. Rev. B* **72** (2005) 174430 (1–8).
29. G. Wiesinger, V. Paul-Boncour, S. M. Filipek, C. Reichl, I. Marchuk, and A. Perchéron-Guegan, *J. Phys.: Condens. Matter* **17** (2005) 893–908.
30. V. Paul-Boncour, S. M. Filipek, A. Perchéron-Guegan, I. Marchuck, and J. Pielaszek, *J. Alloys Compd.* **317**–**318** (2001) 83–87.
31. K. Shashikala, P. Raj, and A. Sathyamoorthy, *Mater. Res. Bull.* **31** (1996) 957–963.
32. V. Paul-Boncour, C. Giorgetti, G. Wiesinger, and A. Perchéron-Guegan, *J. Alloys Compd.* **356**–**357** (2003) 195–199.
33. V. A. Yartys, V. V. Burnasheva, K. N. Semenenko, N. V. Fadeeva, and S. P. Solov'ev, *Int. J. Hydrogen Energy* **7** (1982) 957–965.
34. R. Ramesh and K. V. S. Rama Rao, *J. Alloys Compd.* **191** (1993) 101–105.
35. F. Pourarian, W. E. Wallace, and S. K. Malik, *J. Less–Common Met.* **83** (1982) 95–103.
36. A. L. Shilov, *Russ. J. Inorg. Chem.* **36** (1991) 1256–1261.
37. K. Kanematsu, T. Sugiyama, M. Sekine, T. Okagaki, and K. J. Kobayashi, *J. Less–Common Met.* **147** (1989) 9–18.
38. R. H. Van Essen and K. H. J. Buschow, *J. Less–Common Met.* **70** (1980) 189–198.
39. M. Latroche, V. Paul-Boncour, and A. Perchéron-Guegan, *Z. Phys. Chem.* **179** (1993) 261–268.
40. V. Paul-Boncour, A. Lindbaum, M. Latroche, and S. Heathman, *Intermetallics* **14** (2006) 483–490.
41. E. Gratz, A. Kottar, A. Lindbaum, M. Mantler, M. Latroche, V. Paul-Boncour, M. Acet, Cl. Barner, W. B. Holzapfel, V. Pacheco, and K. Yvon, *J. Phys.: Condens. Matter.* **8** (1996) 8351–8361.
42. A. Perchéron-Guegan, V. Paul-Boncour, M. Latroche, J. C. Achard, and F. Bouree-Vigneron, *J. Less–Common Met.* **172**–**174** (1991) 198–205.
43. A. Slebarski, *J. Less–Common Met.* **141** (1988) L1–L7.
44. A. F. Deutz, R. B. Helmoldt, A. C. Moleman, D. B. de Mooij, and K. H. J. Buschow, *J. Less–Common Met.* **153** (1989) 259–266.
45. M. Latroche, V. Paul-Boncour, A. Perchéron-Guegan, and J. C. Achard, *J. Less–Common Met.* **161** (1990) L27–L31.

46. K. Aoki, A. Kamachi, and T. Masumoto, *J. Non-Cryst. Solids* **61–62** (1984) 679–684.
47. T. Ahiara, K. Aoki, and T. Masumoto, *J. Japan Inst. Metals* **54** (1990) 1189–1196.
48. O. Myakush, Yu. Verbovytsky, I. Saldan, I. Koval'chuck, I. Zavaliy, and B. Kotur, *Physicochem. Mech. Mater.* **6** (2004) 62–66.
49. Yu. Verbovytsky, O. Myakush, A. Soldak, and B. Kotur, *Visnyk Lviv Univ. Ser. Chem.* **46** (2005) 48–52.
50. O. Myakush, G. Martyniuk, Yu. Verbovytsky, and B. Kotur, *Visnyk Lviv Univ. Ser. Chem.* **47** (2006) 25–30.
51. B. Kotur, O. Myakush, and I. Zavaliy, *J. Alloys Compd.* **442** (2007) 17–21.
52. Yu. Verbovytsky, O. Myakush, A. Soldak, B. Kotur, I. Koval'chuck, I. Saldan, and I. Zavaliy, *XIth International Seminar on Physics and Chemistry of Solids,* Czestochowa, 2005, p.11.
53. O. Myakush, Yu. Verbovytsky, B. Kotur, I. Kovalchuk, V. Beresovetz, and I. Zavaliy, *J. Phys.: Conf. Ser.* **79** (2007) 012018.
54. O. R. Myakush, Yu. V. Verbovytsky, V. V. Beresovetz, O. G. Ershova, V. D. Dobrovolsky, and B. Ya. Kotur, *Physicochem. Mech. Mater.* **5** (2007) 76–80.
55. O. R. Myakush, Yu. V. Verbovytsky, I. V. Koval'chuck, R. V. Denys, V. V. Berezovets, and B. Ya. Kotur, *Xth International Conference on Crystal Chemistry of Intermetallic Compounds,* Lviv, Ukraine, 17–20 Sept., 2007, p. 73.
56. B. Kotur, Yu. Verbovytsky, O. Myakush, I. Kovalchuk, and V. Berezovets, *International Conference on Solid Compounds of Transition Elements*, Dresden, July 26–31, 2008, p. 344.
57. A. M. Palasyuk, B. Ya. Kotur, and O. R. Myakush, *International Conference on Phase Diagrams in Materials Science*, Techn. Progr. & Abstr., Kiev, 2001, p. 111.
58. O. R. Myakush, R. V. Denys, I. V. Kovalchuk, Yu. V. Verbovytsky, I. Yu. Zavaliy, and B. Ya. Kotur, *Physicochem. Mech. Mater.* **6** (2003) 77–80.
59. I. Kovalchuk, O. Myakush, R. Denys, and B. Kotur, *Visnyk Lviv. Univ. Ser. Chem.* **48** (2007) 194–197.
60. K. G. Gross, D. Chartouni, and F. Fauth, *J. Alloys Compd.* **306** (2000) 203–218.
61. P. Spatz, K. J. Gross, A. Züttel, and L. Schlapbach, *J. Alloys Compd.* **260** (1997) 211–216.
62. Y. E. Filinchuk, D. Sheptyakov, G. Hilscher, and K. Yvon, *J. Alloys Compd.* **358** (2003) 46–151.
63. S. Rundqvist, R. Tellgren, and Y. Andersson, *J. Less–Common Met.* **101** (1984) 145–168.
64. D. M. Gualtieri and W. E. Wallace, *J. Less–Common Met.* **55** (1977) 53–59.

SAŽETAK

Sposobnost apsorpcije vodika nekih $RM_{2-x}M'_x$ i $RM_{2-x}Al_x$ (R = Y, Gd, Tb, Er, Ho; M = Mn, Fe, Co, Ni) ternarnih Lavesovih faza

Bohdan Kotur,[a] Oksana Myakush[a] i Ihor Zavaliy[b]

[a]*Department of Inorganic Chemistry, Ivan Franko National University of Lviv, Kyryla & Mefodiya Str. 6, UA-79005 Lviv, Ukraine*
[b]*Physico-Mechanical Institute of NAS of Ukraine, Naukova Str. 3, Lviv, UA-79601, Ukraine*

Autori su predočili literaturne i vlastite rezultate istraživanja utjecaja apsorpcije vodika na kristalnu strukturu nekih binarnih RM_2 i ternarnih $RM_{2-x}M'_x$, $R_{1-x}R'_xNi_2$ i $RM_{2-x}Al_x$, (R = rijetke zemlje; M = Mn, Fe, Co, Ni) Lavesovih faza. Apsorpcijom vodika pri sobnoj temperaturi i tlaku 0,1 do 0,12 MPa većina tih spojeva zadržava vlastitu kristalnu strukturu. Lavesove faze tvore hidride koji sadržavaju do 4,2 atoma vodika, a pri visokom tlaku i do 5 atoma vodika na jednu formulsku jedinku. Pritom volumen elementarne ćelije poraste do 20 %, a pri visokom tlaku do 30 %. U brojnim slučajevima dopiranjem binarnih faza trećim elementom pri istim uvjetima tlaka i temperature povećava se sposobnost apsorpcije vodika. Tijekom apsorpcije vodika struktura polaznog spoja ostaje sačuvana ili trpi manju distorziju.